COMMUNICATIONS CHEMISTRY

ARTICLE

https://doi.org/10.1038/s42004-019-0221-5 OPEN

Inducing molecular isomerization assisted by water

Dongsheng Wang[1,2], Lei Zhao[1,3], Haiquan Zhao[1], Jiazun Wu[1], Manfred Wagner[4], Wen Sun[5], Xiaodong Liu[1], Mao-sheng Miao[3] & Yonghao Zheng[1*]

Light is not the only stimulus that can induce *linear*-to-*cyclic* isomerization of donor-acceptor Stenhouse adducts (DASAs). Here we demonstrate the water-induced *linear*-to-*cyclic* isomerization of DASAs. The mechanism of the water-induced *linear*-to-*cyclic* isomerization of DASAs is investigated by density functional theory (DFT) calculations. Water molecules coordinate with DASAs and stabilize the intermediates and *cyclic* isomers, which favors cyclization thermodynamically. Moreover, the *linear*-to-*cyclic* isomerization is reversible. Heating removes the coordinated H_2O molecules, which further triggers *cyclic*-to-*linear* isomerization. DASAs have been applied in information hiding/displaying and color switching under water vapor and heating control.

[1] School of Optoelectronic Science and Engineering, University of Electronic Science and Technology of China, 610054 Chengdu, China. [2] State Key Laboratory of Polymer Materials Engineering, Sichuan University, 610065 Chengdu, China. [3] Department of Chemistry and Biochemistry, California State University Northridge, Northridge, CA 91330-8262, USA. [4] Max-Planck-Institute for Polymer Research, Ackermannweg 10, 55128 Mainz, Germany. [5] State Key Laboratory of Fine Chemicals, Dalian University of Technology, 116024 Dalian, China. *email: zhengyonghao@uestc.edu.cn

Donor-acceptor Stenhouse adducts (DASAs) as novel photoresponsive molecules have been attracting the attention of researchers since 2014[1–8]. DASAs show *linear*-to-*cyclic* isomerization under visible or near-infrared (NIR) light irradiation (~480–750 nm), while *cyclic*-to-*linear* isomerization occurs upon heating in the dark[9]. Light irradiation switches the polarity of DASA molecules. In particular, the DASAs with alkyl-substituted electron-donating moieties show zwitterionic *cyclic* isomers that exhibit higher dipole moments than the *linear* forms[6]. Moreover, the DASAs with aryl-substituted electron-donating moieties show nonzwitterionic *cyclic* isomers[6].

Compared with traditional UV-light-responsive molecules, including azobenzene[10], spiropyran[11], coumarin[12], and *o*-nitrobenzyl molecules[13], DASAs that are responsive to visible or NIR light are attractive, especially for potential applications in biomedicine. In fact, several groups have been working on drug-delivery systems and intelligent surfaces controlled by visible light[14–17].

However, until now, most researches have only focused on the light-induced isomerization. In the current report, we demonstrate the water-induced *linear*-to-*cyclic* isomerization of DASAs, which is reversible under heating. Since the earliest report *cyclic* DASAs have been found to be more stable when water exists[1]. The *linear*-to-*cyclic* isomerization occurs under dark in aqueous environment was also noticed by Feringa's group earlier in 2016 and 2018[18–20]. However, to our knowledge no research is focusing on the mechanism of the water-induced isomerization and the relationships between DASAs and H_2O molecules, which are important for the understanding, development and application of DASAs.

Herein, the mechanistic investigation is guided by density functional theory (DFT) calculations. Water molecules coordinate with DASAs and lower the energy levels of the intermediates and *cyclic* isomer. More importantly, the water-induced process iss demonstrated to be reversible. The *cyclic*-to-*linear* isomerization is induced by removing the coordinated H_2O molecules (Fig. 1). DASAs are further applied in information hiding/displaying and color switching under controlling of water vapor and heat exposure.

Results

Water-induced *linear*-to-*cyclic* isomerization of DASAs. DASA-N, DASA-O with zwitterionic *cyclic* isomers and DASA-M, DASA-I with nonzwitterionic *cyclic* isomers were synthesized (Fig. 1 and Supplementary Fig. 1)[1,4,6]. *Linear*-to-*cyclic* isomerizations triggered by green light (530 nm) were observed for all DASAs (Fig. 2a and Supplementary Figs. 2–5). Colorless *cyclic* DASA-N was obtained after irradiation, and this species is unstable in toluene (Fig. 2a). Interestingly, after adding water into a toluene solution of *linear* DASA-N (toluene:water = 6:1, v/v), we found that the *linear* DASA-N spontaneously converts to *cyclic* DASA-N, even without light, this is in good accordance to the previous reports (Fig. 2b)[1,2,18–20]. The process is extremely slow compared with the light-induced isomerization, and only ~30% of *cyclic* DASA-N can be obtained after 10 h, and the process is finished in 40 h (Supplementary Fig. 7). Furthermore, the *cyclic* DASA-N is stabilized by H_2O molecules, and therefore, it does not switch back to the *linear* isomer during ^1H NMR studies (Fig. 2c). The results were supported by 2D ^1H-^1H chemical shift correlation spectroscopy (2D-COSY) (Supplementary Figs. 8–10).

These results indicated that in addition to light, water is also able to trigger the *linear*-to-*cyclic* isomerization of DASA-N. Importantly, the rate of the water-induced *linear*-to-*cyclic* isomerization is positively correlated with the temperature. The isomerization of DASA-N was investigated at 4, 20, and 40 °C (Supplementary Figs. 11–13). We learned that higher temperatures resulted in faster *linear*-to-*cyclic* isomerization rates (Fig. 2c). The water-induced isomerization of DASA-N was demonstrated to be a thermal process, which is similar to the thermal-induced *cis*-to-*trans* isomerization of azobenzene and water-induced *spirocyclic*-to-*merocyanine* isomerization of spiropyran (Fig. 2d, see the SI for details)[21,22]. As expected, the rate constant for the *linear*-to-*cyclic* isomerization of DASA-N at 40 °C is two orders of magnitude higher than that at 4 °C (Fig. 2d). In other words, *cyclic* DASA-N may be stabilized in the presence of water.

In addition to DASA-N, water-induced *linear*-to-*cyclic* isomerizations were observed for DASA-O, DASA-M and DASA-I (Supplementary Figs. 14–16)[7]. For both of the DASA molecules with zwitterionic *cyclic* isomers (DASA-N and DASA-O) and nonzwitterionic *cyclic* isomers (DASA-M and DASA-I), more than 60% of the *linear* isomers converted to the *cyclic* isomers after 90 min of heating at 40 °C (Supplementary Figs. 17–20). All the DASA molecules show similar isomerization rates, indicating the universality of the water-induced *linear*-to-*cyclic* isomerization in both of the DASA molecules with zwitterionic and nonzwitterionic *cyclic* isomers (Supplementary Fig. 21).

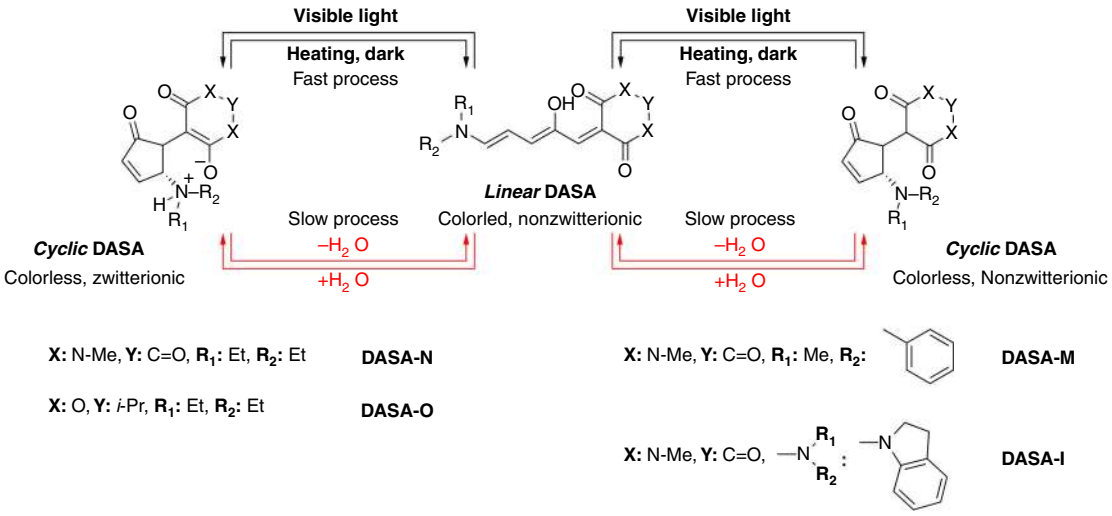

Fig. 1 Light-induced and water-induced isomerization. Schematic illustration of light-induced (previously reported) and water-induced (this work) *linear*-to-*cyclic* isomerizations of DASAs

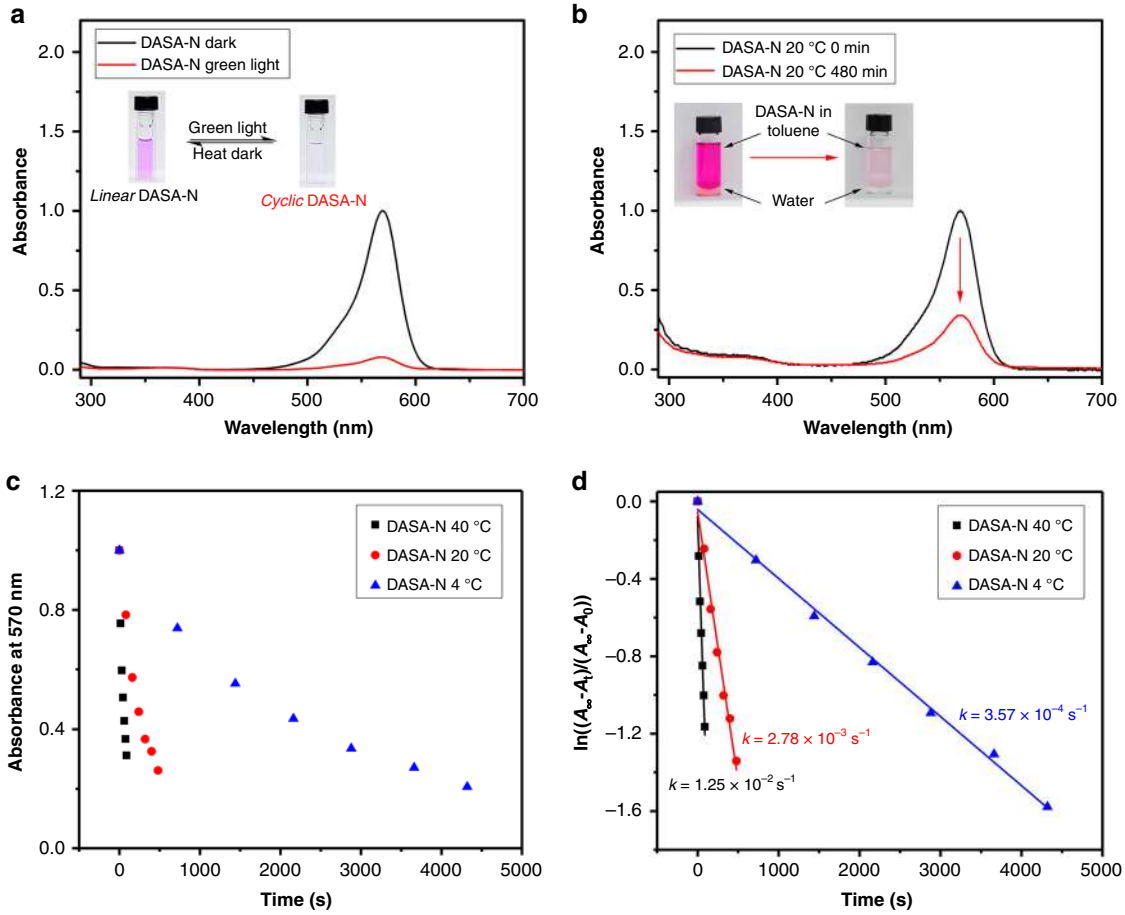

Fig. 2 Molecular isomerization of DASA-N. **a** UV/vis spectra of DASA-N in the dark (black) and after irradiation with green light (red) ([DASA-N] = 0.04 mM in toluene); **b** UV/vis spectra of DASA-N after water treatment at 20 °C for 0 min (black) and 480 min (red) ([DASA-N] = 0.04 mM in toluene, toluene:water = 6:1, v/v) (Due to toluene and water are not miscible, the water concentration in toluene is ~27 mM); **c** Time-dependent change in absorbance (570 nm) of DASA-N under water treatment at 40 °C (black, square), 20 °C (red, circle), and 0 °C (blue, triangle) ([DASA-N] = 0.04 mM in toluene, toluene:water = 6:1, v/v); **d** Plot of kinetic absorption data of DASA-N under water treatment at 40 °C (black, square), 20 °C (red, circle), and 0 °C (blue, triangle) ([DASA-N] = 0.04 mM in toluene, toluene:water = 6:1, v/v). The absorbance at 568 nm is normalized

DASAs are not the only photoresponsive molecules that show water-induced isomerization. Solvents have been reported to favor the isomerization of photoresponsive molecules (e.g., azobenzene and spiropyran) and affect the isomer distribution[23,24], and this is especially true for spiropyrans with zwitterionic *merocyanine* isomers. H_2O molecules are believed to form hydrogen bonds with the *merocyanine* spiropyran, lowering its ground state energy, which allows the *spirocyclic*-to-*merocyanine* isomerization in the absence of light[21].

Mechanism of the water-induced isomerization. DFT calculations were applied to investigate the mechanism of the water-induced *linear*-to-*cyclic* isomerization of the DASAs. The kinetic investigation indicated that the *cyclic* DASA may be stabilized by H_2O molecules and show a lower ground state energy. Therefore, H_2O molecules are assumed to coordinate with DASAs in toluene.

Up to 5 H_2O molecules can form complexes with DASA-N (Fig. 3a **and** Supplementary Fig. 27). The H_2O molecules are arranged between the hydroxyl and carbonyl groups of *linear* DASA-N due to hydrogen bonding (Supplementary Fig. 28). All the possible positions for coordinating of water molecules are investigated (Supplementary Figs. 29–39, Supplementary Tables 1, 2). For *cyclic* DASA-N, the H_2O molecules stably surround the carbonyl in the electron-withdrawing domain (Fig. 3a). Molecular dynamics (MD) simulations indicated that the binding between H_2O molecules and *cyclic* DASA-N is stronger than that with *linear* DASA-N. All the *linear* DASA-N·xH_2O ($x = 1$–5) were dissociated after 9 ps MD simulations, while the molecular geometries were stable under the same conditions for *cyclic* DASA-N·xH_2O ($x = 3$ and 5) (Supplementary Figs. 40–45). These results indicated *cyclic* DASA-N could be stabilized by H_2O molecules.

Similar results were concluded by calculating the energy difference (ΔE) between the *linear* and *cyclic* isomers ($E_{cyclic} - E_{linear}$), which shows a decreased ΔE as the number of surrounding H_2O molecules increases (Fig. 3b and Supplementary Table 3). The ΔE goes to the lowest when 3 H_2O molecules coordinate with DASA-N, indicating that the *cyclic* DASA-N is stabilized by H_2O molecules (Fig. 3b, c). However, by further increasing the number of coordinated H_2O molecules (DASA-N·4H_2O and DASA-N·5H_2O), the ΔE does not further decrease (Fig. 3b and Supplementary Table 3). These results are in good accordance with MD simulations.

Similar results were noticed by applying water as the solvent. Actually, the ΔE is negative when applying water as the solvent, which is thermodynamically favorable for the *linear*-to-*cyclic* isomerization of DASA-N (Supplementary Figs. 46, 51 and Supplementary Table 4). Moreover, for the *cyclic* DASA-N, the

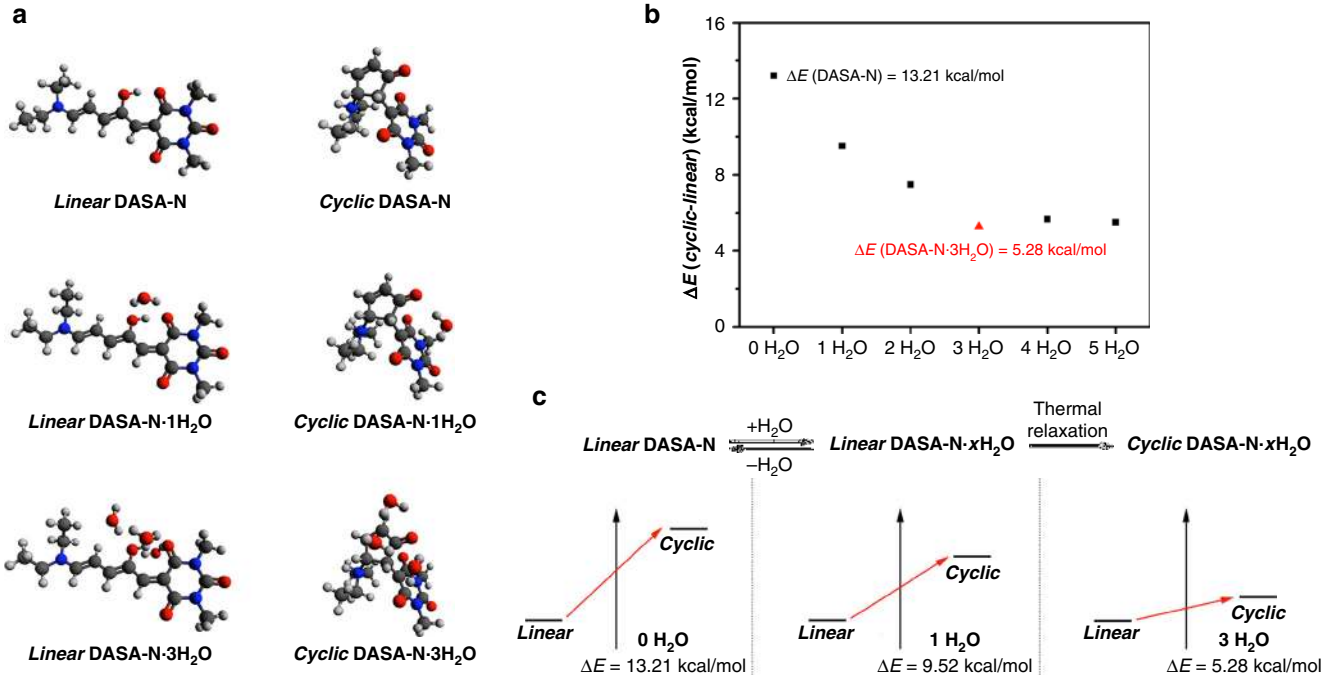

Fig. 3 DFT calculations. **a** Molecular structures of DASA-N coordinated with 0, 1, and 3 H_2O molecules by DFT. Full geometry optimizations were carried out at the M06-2X/6–311++g(d, p) level of theory, and toluene was selected as the solvent. **b** ΔE between the *linear* and *cyclic* DASA-N coordinated to various numbers of H_2O molecules. **c** Schematic illustration of the putative mechanism of the water-induced *linear*-to-*cyclic* isomerization of DASA-N

coordinated H_2O molecules may transfer to quaternary ammonium salt in the electron-donating domain, which further lowers the ΔE (Supplementary Fig. 47, 52 and Supplementary Table 5). Therefore, for the thermodynamic concern, water molecules play two roles during the *linear*-to-*cyclic* isomerization of DASA-N: (1) water molecules coordinated around the hydroxyl and carbonyl decrease ΔE between *linear* and *cyclic* DASA-N, which favors the *linear*-to-*cyclic* isomerization; (2) water molecules coordinated on quaternary ammonium salt further decrease the molecular energy and stabilize *cyclic* DASA-N. In this work, all the coordinated H_2O molecules were set around the carbonyl in the electron-withdrawing domain for a direct comparison.

Similar results were observed for DASA-O, DASA-M and DASA-I through DFT calculations (Supplementary Figs. 48–50). H_2O molecules coordinate with DASAs through hydrogen bonding to stabilize the *cyclic* isomers (Supplementary Figs. 53–55 and Supplementary Table 6–8). However, for DASA-M, even without H_2O molecules, the *linear* isomers are not more stable than the *cyclic* isomers (Supplementary Fig. 54). Considering that isomerization only occurs in the presence of water, the process of the water-induced *linear*-to-*cyclic* isomerization was investigated.

Feringa's group demonstrated a intermediates-included *linear*-to-*cyclic* isomerization process of DASAs[18,20,25]. *Linear* DASAs (A1) switches to A2 via a light-induced C–C isomerization (Fig. 4a). Afterwards, A2 switches to A3 via a thermal-induced C–C rotation, and through a A2-A3 transition state. A3 then switches to *cyclic* DASAs (A4) through the cyclization (Supplementary Fig. 56). The Gibbs free energy of the intermediates of DASA-N were calculated by DFT methods (see the Supplementary Methods for details). With the process of *linear*-to-*cyclic* isomerization, the free energy of DASA-N increases step by step, and reaches the highest for A4 (Fig. 4c). These results are in good accordance with the previous reports[25]. After coordinated with 3 H_2O molecules, the *linear*-to-*cyclic* isomerization is induced by thermal (Fig. 4b). The Gibbs free energy decreases step by step with the process, which thermodynamically favors the *linear*-to-*cyclic* isomerization of DASA-N·3H_2O (Fig. 4d). These results also explain why the *cyclic*-to-*linear* isomerization of DASA-N·3H_2O does not occur spontaneously. The process of *linear*-to-*cyclic* isomerization of DASA-M and DASA-M·3H_2O is similar to DASA-N and DASA-N·3H_2O (Fig. 4a, b). H_2O molecules coordination causes a decreased free energy of the intermediates, which favors the isomerization (Fig. 4c, d).

Moreover, previous research demonstrated that an intramolecular proton transfer mechanism was involved in the light-induced *linear*-to-*cyclic* isomerization of DASAs[19]. Protons transfer from the hydroxyl group to the carbonyl group, which favors cyclization (Supplementary Fig. 58). Moreover, Feringa's group very recently reported that protic solvents mainly affect the thermal process in the light-induced *linear*-to-*cyclic* isomerization[11]. In this work, we hypothesized the coordinated H_2O molecules could assist in the intramolecular proton transfer from the hydroxyl group to the carbonyl group (Supplementary Fig. 58), further promoting the cyclization (Fig. 58, B3–B4).

Heat-induced *cyclic*-to-*linear* isomerization of DASAs. The water-induced *linear*-to-*cyclic* isomerization of DASA is reversible. Removing the coordinated H_2O molecules induces *cyclic*-to-*linear* isomerization. The *cyclic* DASA-N·xH_2O was prepared in two steps, namely, heating the mixture of *linear* DASA-N and water at 70 °C, and then gently evaporating the solvent (see the SI for details). Anhydrous $MgSO_4$ and a microwave oven were tested for removing the coordinated H_2O molecules. However, no *cyclic*-to-*linear* isomerization was observed by UV-vis, indicating that the complexes are stable. Actually, *cyclic* DASA-N·xH_2O does not switch back to *linear* DASA-N in DCM (Supplementary Fig. 59). The thermal gravimetric analysis (TGA) curves of the *cyclic* DASA-N·xH_2O showed that weight loss began at 145 °C, which can be attributed to the loss of coordinated H_2O molecules (Fig. 5a). In contrast, the *linear* DASA-N begins to lose weight at 224 °C and almost reaches equilibrium at 500 °C. The number of

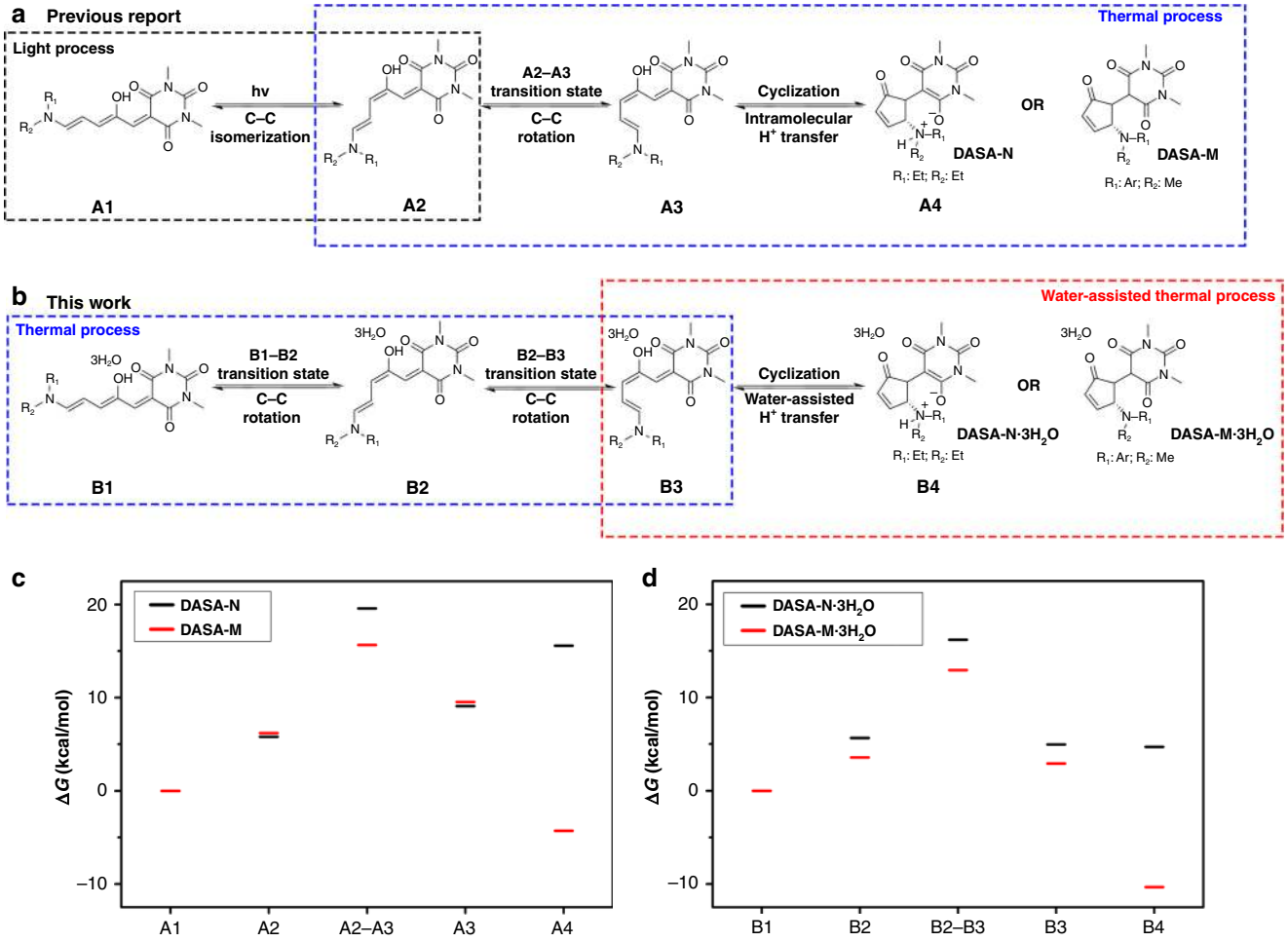

Fig. 4 Investigation of linear-to-*cyclic* isomerization process. **a** Schematic illustration of the reported mechanism of the light-induced *linear*-to-*cyclic* isomerization of DASA-N and DASA-M. **b** Schematic illustration of the hypothesized mechanism of the water-induced *linear*-to-*cyclic* isomerization of DASA-N·3H_2O and DASA-M·3H_2O. **c** Relative Gibbs energy levels of DASA-N and DASA-M in toluene. **d** Relative Gibbs energy levels of DASA-N·3H_2O and DASA-M·3H_2O in toluene

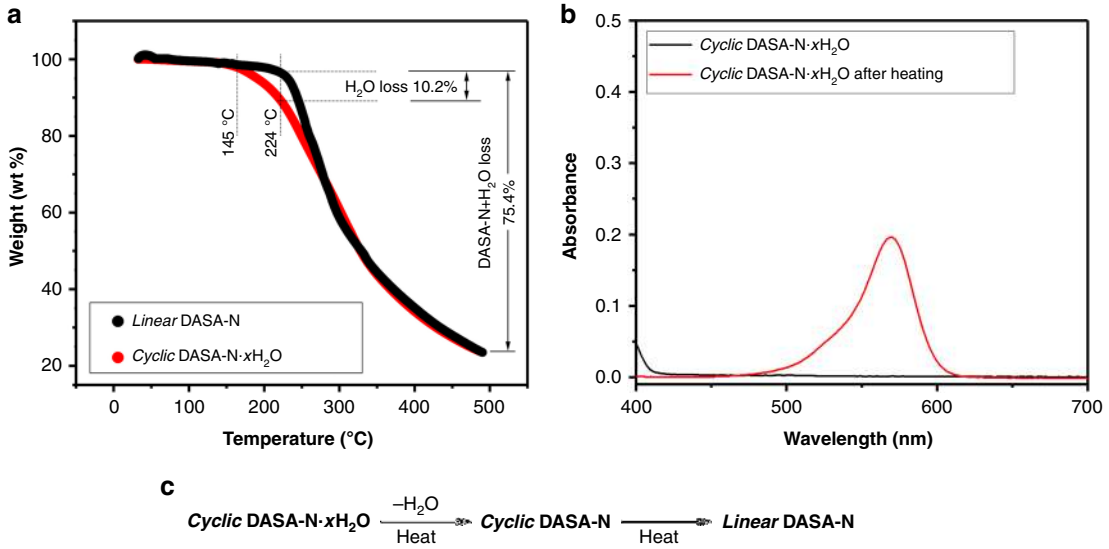

Fig. 5 *Cyclic*-to-*linear* isomerization. **a** Thermal gravimetric analysis curves for linear DASA-N (black) and cyclic DASA-N·xH_2O (red). **b** UV/vis spectra of cyclic DASA-N·xH_2O before (black) and after (red) heating ([DASA-N] = 0.04 mM in dichloromethane (DCM)). **c** Putative mechanism of the *cyclic*-to-*linear* isomerization of DASA-N induced by removing the coordinated H_2O molecules

H_2O molecules (x) coordinated to the *cyclic* DASA-N·xH_2O was calculated to be >2.6, which is in good agreement with the DFT results (Fig. 5a).

We tried to heat the *cyclic* DASA-N·xH_2O to remove the coordinated H_2O molecules. A droplet of a colorless solution of *cyclic* DASA-N·xH_2O in methanol (0.1 mM) was dropped on filter paper. After heating with a heat gun at 180 °C for ~10 s, the colorless spot on the filter paper became bright purple (Supplementary Fig. 61). UV/vis spectra of *cyclic* DASA-N·xH_2O showed a sharp increase of the absorbance in visible region after heating, indicating the formation of *linear* DASA-N (Fig. 5b). These were further demonstrated by ^{1}H NMR and Fourier transform infrared (FTIR) spectra (Supplementary Figs. 65, 66). Therefore, heating can remove the coordinated H_2O molecules of *cyclic* DASA-N·xH_2O, and further triggers the *cyclic*-to-*linear* isomerization (Fig. 5c). DASA-N is reversible in 5 *linear*-to-*cyclic* and *cyclic*-to-*linear* cycles, and thermally stable under 180 °C (Supplementary Figs. 67, 68). The reversible isomerization of DASA-N by adding and removing coordinated H_2O molecules is important for DASAs, which are potential to be applied as hydrochromic and thermochromic molecules.

The *cyclic*-to-*linear* isomerization triggered by removing the coordinated H_2O molecules occurs for all the DASA-N, DASA-O, DASA-M and DASA-I, indicating the universality of the phenomena (Supplementary Figs. 62–64, 72, 73).

Application in information hiding/displaying and color-switched inks. Due to the reversibility of the water-induced *linear*-to-*cyclic* isomerization, DASA-N was applied in information hiding/displaying and color switching under controlling of water vapor and heat exposure (Fig. 6). A "9" was written on filter paper using normal purple pigment, and a vertical line was added with the DASA-N ink ([DASA-N] = 0.3 mM in dichloromethane) to form an "8" (Fig. 6a). Water vapor treatment switched the *linear* DASA-N to colorless *cyclic* DASA-N, changing the "8" to a "9" (Fig. 6a and Supplementary Movie 1). The *cyclic* DASA-N is stable on filter paper under ambient conditions for months and does not switch back to the *linear* form. Heating at 180 °C for ~30 s removed the coordinated H_2O molecules and changed the "9" back to an "8" (Fig. 6a and Supplementary Movie 2).

By mixing the DASA-N with stimuli-nonresponsive dyes, color switching can be achieved by controlling exposure to vapor and heating (Fig. 6b). DASA-N and azure II were dissolved in dichloromethane ([DASA-N] = 0.3 mM, [azure II] = 0.2 mM) to prepare color-switching ink. The smiley face on the filter paper switched from purple to cyan after water vapor treatment for ~5 min due to the water-induced *linear*-to-*cyclic* isomerization of DASA-N (Fig. 6b and Supplementary Movie 3). Heating at 180 °C triggered the *cyclic*-to-*linear* isomerization and switched the smiley face back to purple in ~30 s (Fig. 6b and Supplementary Movie 4). Peak shifting at visible light region was observed for the DASAs/azure II color-switched inks, which is reversible for several cycles after sequential treatment of vapor and heat (Fig. 6c, d). Moreover, a series of color-switching inks were prepared by mixing DASA-N with various stimuli-nonresponsive dyes, including dimethyl yellow, methylene blue, Fast Green FCF, and methyl violet (Supplementary Figs. 74, 75, see the SI for details).

Discussion

In summary, we report the reversible, water-induced *linear*-to-*cyclic* isomerization of DASAs. Both the DASAs with zwitterionic

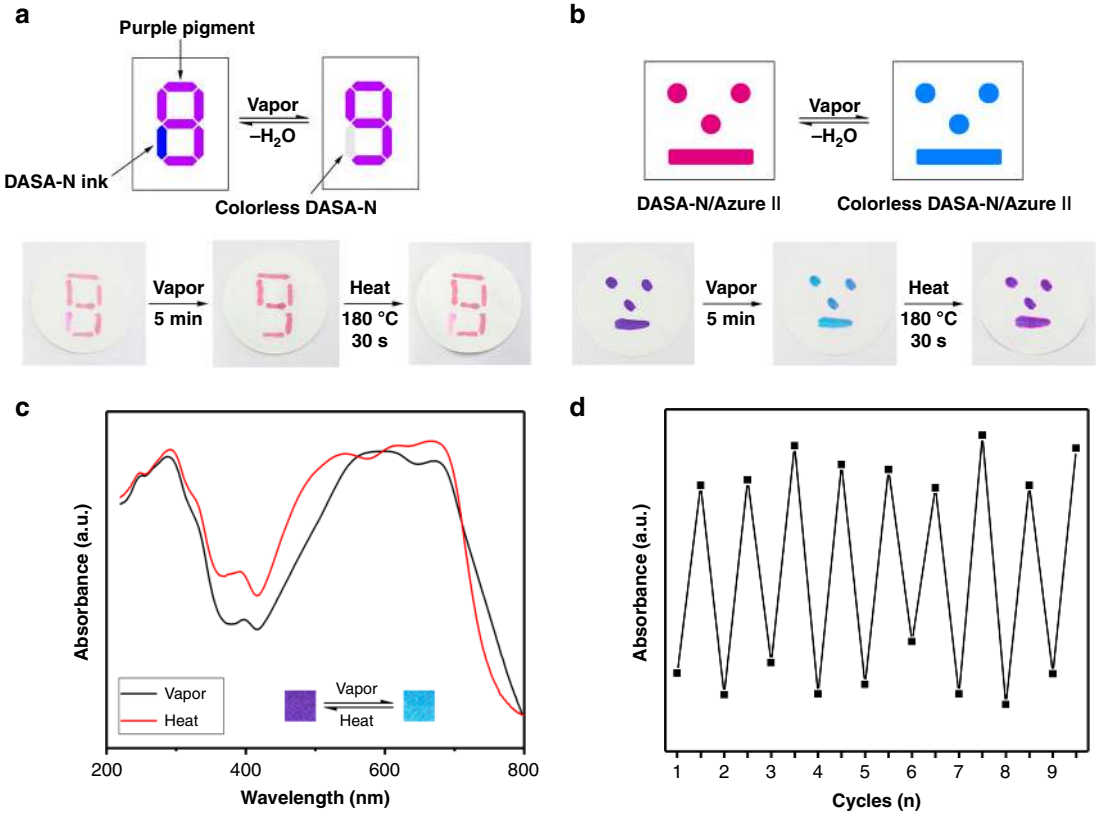

Fig. 6 Applications of water-induced isomerization of DASAs. **a** Schematic illustration and photographs of switching between "8" and "9" using DASA-N under controlling of water vapor and heat exposure. **b** Schematic illustration and photographs of switching the color between purple and cyan by DASA-N under controlling of water vapor and heat exposure. **c** UV/vis spectra of color-switched inks on paper after treating with vapor (black) and heat (red). Insert shows the color change. **d** Absorbance (500 nm) of color-switched inks on paper after sequential vapor and heat treating

(i.e., DASA-N and DASA-O) and nonzwitterionic (i.e., DASA-M and DASA-I) *cyclic* isomers show water-induced *linear*-to-*cyclic* isomerizations. The isomerization process is positively correlated with temperature. H_2O molecules coordinate with the DASAs and stabilize their *cyclic* isomers. Approximately three H_2O molecules coordinate with the DASA-N and switch the *linear* isomer to the colorless and stable *cyclic* DASA-N·xH_2O. Removing the coordinated H_2O molecules by heating induces the *cyclic*-to-*linear* isomerization of DASAs, indicating that the water-induced process is reversible. The DASA-N was applied in information hiding/displaying and color-switched inks under controlling of water vapor and heating exposure.

As DASAs are reported as novel photoresponsive molecules, the investigations of their applications are still in their infancy. In addition to the light-induced process, the reported reversible water-induced *linear*-to-*cyclic* isomerization deepens our understanding and broadens the applications of the DASAs. Therefore, the role of H_2O molecules to induce *linear*-to-*cyclic* isomerization of DASAs is encouraged to be understood from different perspective and needs further researches. We envision that DASAs can be widely applied in supramolecular materials, energy and printing applications based on the water-induced process. Light and water can be used to switch the DASAs in an orthogonal manner[3,26]. Moreover, DASAs that are responsive to visible or even NIR light have the potential to be applied in biomedicine[27]. Therefore, in this case, limiting the water-induced *linear*-to-*cyclic* isomerization is important. Understanding the mechanism of the water-induced process is thus helpful for synthesizing a DASA that is stable in water and is only responsive to light.

Methods

General synthesis of DASAs. Step I: electron-withdrawing part (Meldrum's acid or 1,3-dimethylbarbituric acid) (1 euqiv.) and furfural (1 equiv.) were dissolved in water. The solution was stirred under room temperature for 2 h. The yellow crude product was filtrated out and washed with cold water two times. Then the precipitate was collected and dissolved into DCM, and washed with saturated $NaHSO_3$ solution, saturated NaCl solution and water sequentially. After drying with MgSO4, the yellow solid was further purified by chromatography to obtain product 1 or 2 (Supplementary Fig. 1).

Step II: product 1 or 2 (1 equiv.) and electron-donating part (diethylamine, *N*-methylaniline or indoline) (1 equiv.) were dissolved in DCM. The mixed solution was stirred under 30 °C for 2 h. After removing the solvent by a rotavapor, the rough product was purified by chromatography to obtain DASAs (Supplementary Fig. 1).

DFT calculations. All the DFT calculations were performed with Gaussian 16 package. Full geometry optimizations were carried out at M06-2X/6–31++g(d,p) level of theory, whereas the reaction pathways were obtained with 6–311++G(d,p) atomic basis set after a basis set test (Supplementary Fig. 22). The choice of this combination was used by several previous benchmarks that demonstrated their performances for weak interactions like hydrogen bonds[18,20,28]. Vibration frequencies were calculated to confirm if all of the structures optimized were at stationary points or true minima on the potential energy surfaces. The solvation model density (SMD) solvation model was chosen to calculate the electronic energy in solution. To describe the hydrogen bonding interaction between SA and water molecules, various number of water molecules (1–5) were modeled and optimized with DASA molecules, and also the obtained stationary points were characterized by frequency calculations. Further data can be found in Supplementary Data 1.

MD simulations. Ab initio molecular dynamics simulations (AIMD) were performed using first-principles DFT as implemented in the Vienna ab initio simulation package (VASP)[29–31]. The exchange and correlation were obtained within the generalized gradient approximation (GGA), using the functional of Perdew, Burke, and Ernzerhof (PBE)[32]. The projector augmented wave (PAW) method was used to describe the potential of the nuclear and the core[33,34]. For the electronic structure calculations, plane waves with a kinetic energy cutoff of 500 eV were adopted to expand the valance electron ($2s^22p^2$) wavefunctions. Brillouin zone (BZ) integrations were carried using Γ centered sampling grids with $1 \times 1 \times 1$. Structural relaxation was performed using the conjugate gradients (CG) scheme until the force components were converged to within 0.02 eV/Å, and the self-consistent field calculations were stopped when the energy difference between two steps was smaller than 1×10^{-6} eV/atom. Temperature was set to 300 K and volume (NVT) were performed to exam thermal stability.

Mass-production of cyclic DASA·xH_2O. *Linear* DASAs were mixed with water. The mixture was heated to 70 °C for 5 h to obtain clear light brown solution. After removing the solvent smoothly by a rotavapor under room temperature, the solid *cyclic* DASA·xH_2O could be obtained.

Data availability

The authors declare that the data supporting the findings of this study are available within the paper and its supplementary information files.

Received: 3 April 2019; Accepted: 25 September 2019;
Published online: 17 October 2019

References

1. Helmy, S. et al. Photoswitching using visible light: a new class of organic photochromic molecules. *J. Am. Chem. Soc.* **136**, 8169–8172 (2014).
2. Helmy, S. et al. Design and synthesis of donor-acceptor Stenhouse adducts: a visible light photoswitch derived from furfural. *J. Org. Chem.* **79**, 11316–11329 (2014).
3. Lerch, M. M. et al. Orthogonal photoswitching in a multifunctional molecular system. *Nat. Commun.* **7**, 12054–12063 (2016).
4. Hemmer, J. R. et al. Tunable visible and near infrared photoswitches. *J. Am. Chem. Soc.* **138**, 13960–13966 (2016).
5. Hemmer, J. R. et al. Controlling dark equilibria and enhancing donor-acceptor Stenhouse adduct photoswitching properties through carbon acid design. *J. Am. Chem. Soc.* **140**, 10425–10429 (2018).
6. Mallo, N. et al. Photochromic switching behavior of donor-acceptor Stenhouse adducts in organic solvents. *Chem. Commun.* **52**, 13576–13579 (2016).
7. Mallo, N. et al. Structure-function relationships of donor-acceptor Stenhouse adduct photochromic switches. *Chem. Sci.* **9**, 8242–8252 (2018).
8. Lerch, M. M. et al. The (photo)chemistry of stenhouse photoswitches: guiding principles and system design. *Chem. Soc. Rev.* **47**, 1910–1937 (2018).
9. Mason, B. P. et al. A temperature-mapping molecular sensor for polyurethane-based elastomers. *Appl. Phys. Lett.* **108**, 041906 (2016).
10. Bandara, H. M. D. & Burdette, S. C. Photoisomerization in different classes of azobenzene. *Chem. Soc. Rev.* **41**, 1809–1825 (2012).
11. Klajn, R. Spiropyran-based dynamic materials. *Chem. Soc. Rev.* **43**, 148–184 (2014).
12. Tunc, D. et al. Reversible cross-linking of aliphatic polyamides bearing thermos- and photoresponsive cinnamoyl moieties. *Macromolecules* **47**, 8247–8254 (2014).
13. Yan, B. et al. Near infrared light triggered release of biomacromolecules from hydrogels loaded with upconversion nanoparticles. *J. Am. Chem. Soc.* **134**, 16558–16561 (2012).
14. Poelma, S. O. et al. Controlled drug release to cancer cells from modular one-photon visible light-responsive micellar system. *Chem. Commun.* **52**, 10525–10528 (2016).
15. Singh, S. et al. Spatiotemporal photopatterning on polycarbonate surface through visible light responsive polymer bound DASA compounds. *ACS Macro Lett.* **4**, 1273–1277 (2015).
16. Zhao, H. Q. et al. Surface with reversible green-light-switched wettability by donor-acceptor Stenhouse adducts. *Langmuir* **34**, 15537–15543 (2018).
17. Sinawang, G. et al. Polystyrene based visible light responsive polymer with donor-acceptor stenhouse adduct pendants. *Macromol. Chem. Phys.* **217**, 2409–2414 (2016).
18. Lerch, M. M. et al. Unraveling the photoswitching mechanism in donor-accepotor stenhouse adducts. *J. Am. Chem. Soc.* **138**, 6344–6347 (2016).
19. Lerch, M. M. et al. Tailoring photoisomerization pathways in donor-acceptor Stenhouse adducts: the role of the hydroxy group. *J. Phys. Chem. A* **122**, 955–964 (2018).
20. Lerch, M. M. et al. Solvent effects on the actinic step of donor-acceptor Stenhouse adduct photoswitching. *Angew. Chem. Int. Ed.* **57**, 8063–8068 (2018).
21. Shiraishi, Y. et al. Thermal isomerization of spiropyran to merocyanine in aqueous media and its application to colorimetric temperature indication. *Phys. Chem. Chem. Phys.* **12**, 13737–13745 (2010).
22. Rau, H. Spectroscopic properties of organic Azo compounds. *Angew. Chem., Int. Ed. Engl.* **12**, 224–235 (1973).
23. Burke, K. et al. Thermosolvatochromism of nitrospiropyran and merocyanine free and bound to cyclodextrin. *J. Phys. Chem. B* **116**, 2483–2491 (2012).
24. Minkin, V. I. et al. Photo-, thermo-, solvato-, and electrochromic spiroheterocyclic compounds. *Chem. Rev.* **104**, 2751–2776 (2004).
25. Donato, M. D. et al. Shedding light on the photoisomerization pathway of donor-acceptor Stenhouse adducts. *J. Am. Chem. Soc.* **139**, 15596–15599 (2017).
26. Wang, D. et al. Orthogonal photo-switching of supramolecular patterned surfaces. *Chem. Commun.* **54**, 3403–3406 (2018).

27. Jia, S. et al. Photoswitchable molecules in long-wavelength light-responsive drug delivery: from molecular design to applications. *Chem. Mater.* **30**, 2873–2887 (2018).
28. Laurent, A. D. et al. Using time-dependent density functional theory to probe the nature of donor-acceptor stenhouse adduct photochromes. *ChemPhysChem* **17**, 1846–1851 (2016).
29. Kohn, W. & Jeu, S. L. Self-consistent equations including exchange and correlation effects. *Phys. Rev.* **140**, A1133–A1138 (1965).
30. Kresse, G. et al. Efficiency of ab-initio total energy calculations for metals and semiconductors using a plane-wave basis set. *Comput. Mater. Sci.* **6**, 15–50 (1996).
31. Kresse, G. & Jürgen, F. Efficient iterative schemes for ab initio total-energy calculations using a plane-wave basis set. *Phys. Rev. B* **54**, 11169–11186 (1996).
32. Perdew, J. P. et al. Generalized gradient approximation made simple. *Phys. Rev. Lett.* **77**, 3865–3868 (1996).
33. Blöchl, P. E. Projector augmented-wave method. *Phys. Rev. B* **50**, 17953–17979 (1994).
34. Kresse, G. et al. From ultrasoft pseudopotentials to the projector augmented-wave method. *Phys. Rev. B.* **59**, 1758–1775 (1999).

Acknowledgements

We would like to thank D. Vollmer (Max-Planck-Institute for Polymer Research) and C. Zhao (College of Polymer Science and Engineering, Sichuan University) for their kind supports and discussions. We would also acknowledge C.He, W.Zhao (College of Polymer Science and Engineering, Sichuan University), and C.Xie (Max-Planck-Institute for Polymer Research) for their help in the measurements of NMR. We gratefully acknowledge the financial support from the National Key R & D Program (2018YFA0307400) and Opening Project of State Key Laboratory of Polymer Materials Engineering (Sichuan University) (Grant No. sklpme2018-4-28).

Author contributions

D.W. and Y.Z. conceived the project and designed the experiments. H.Z. contributed to the synthesis of the DASAs. L.Z. and M-S.M.contributed to the DFT calculation of DASAs. J.W. and X.L. designed, prepared and measured the organic solar cells. M-S. W. and W.S. measured and analyzed the NMR data. D.W. and Y.Z. analyzed the data and co-wrote the paper. All authors discussed the results and commented on the paper.

Competing interests

The authors declare no competing interests.

Additional information

Supplementary information is available for this paper at https://doi.org/10.1038/s42004-019-0221-5.

Correspondence and requests for materials should be addressed to Y.Z.

Reprints and permission information is available at http://www.nature.com/reprints

Publisher's note Springer Nature remains neutral with regard to jurisdictional claims in published maps and institutional affiliations.